Ecological Informatics 95 (2026) 103718

Contents lists available at ScienceDirect

Ecological Informatics

journal homepage: www.elsevier.com/locate/ecolinf

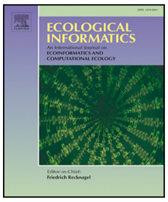

Development and implementation of a passive surveillance system for *Aedes albopictus* in Emilia-Romagna, Italy

Margo Blaha [a,*], Alessandro Albieri [b], Paola Angelini [c], Gabriele Antolini [d], Carmelo Bonannella [e], Fabrizio Laurini [f], Roberto Rosà [a,1], Daniele Da Re [a,g,1]

[a] *Center Agriculture Food Environment, University of Trento, S. Michele all'Adige, Italy*
[b] *Centro Agricoltura Ambiente "G.Nicoli", Crevalcore, Italy*
[c] *Emilia Romagna region, Bologna, Italy*
[d] *Regional Agency for Prevention, Environment and Energy of Emilia-Romagna, HydroMeteoClimate Service (ARPAE-SIMC), Viale Silvani 6, 40122 Bologna, Italy*
[e] *OpenGeoHub Foundation, Doorwerth, The Netherlands*
[f] *Department of Economics and Management, University of Parma, Parma, Italy*
[g] *Research and Innovation Centre, Fondazione Edmund Mach, S. Michele all'Adige, Italy*

ARTICLE INFO

Dataset link: www.github.com/margoblaha/StackedER

Keywords:
Ecological forecasting
Invasive mosquito
Public health
Species distribution modelling
Vector-borne diseases

ABSTRACT

The invasive Asian tiger mosquito (*Aedes albopictus*) is a major public health concern in Italy, particularly in the Po Valley, where it has contributed to repeated outbreaks of mosquito-borne diseases over the past two decades. In response, the Emilia-Romagna region (Northern Italy) has maintained an intensive surveillance program based on oviposition traps since 2010, generating a rich long-term observational dataset for this invasive species.

This study aims to develop a forecasting model that estimates abundance at both monitored and unmonitored locations, directly supporting regional mosquito control efforts. We implemented a stacked machine learning framework to forecast weekly *Ae. albopictus* distribution and abundance using ovitrap data and ecologically relevant environmental covariates, with the aim of quantifying spatial and temporal data needs under realistic surveillance constraints. Therefore, we evaluate model performance across a structured set of training-window configurations that vary both the temporal depth and the spatial coverage of the input data.

Our evaluation across configurations reveals that broader spatial coverage can compensate for a shorter recent temporal window. Configurations spanning only two recent years but incorporating more sampling locations matched or exceeded the predictive performance of configurations with longer historical records, suggesting that recency and spatial breadth are important for forecasting under stable environmental conditions. Regardless of the training-window scenario, all models consistently reproduced the seasonal and spatial patterns of *Ae. albopictus*. These findings offer practical guidance for designing operational mosquito surveillance and forecasting systems and support the use of abundance-based predictions to inform public health planning and vector control strategies.

1. Introduction

The Asian tiger mosquito, *Aedes albopictus* (Skuse, 1894), is a vector of arboviruses such as Chikungunya, Dengue, and Zika, and it is also one of the most rapidly spreading invasive species in the world (Benedict et al., 2007; Delatte et al., 2008; Boes et al., 2014; Kraemer et al., 2015). Due to its ability to establish in new environments and transmit pathogens (Benedict et al., 2007), its rapid spread across Italy has raised significant public health concerns and required robust surveillance and control strategies (Rezza et al., 2007; Venturi et al., 2017; Brady and Hay, 2019; Barzon et al., 2021; De Carli et al., 2023; Branda et al., 2024; Sacco et al., 2024). The urgency of this issue was exemplified by the response of the Emilia-Romagna region (Italy) to the 2007 Chikungunya outbreak, which underscored the need for efficient and targeted monitoring systems to prevent future epidemics (Canali et al., 2017; Angelini et al., 2008). However, implementing such systems using traditional surveillance methods requires substantial financial

---

[*] Corresponding author.
E-mail address: margo.blaha@unitn.it (M. Blaha).
[1] Shared senior authorship.

https://doi.org/10.1016/j.ecoinf.2026.103718
Received 21 March 2025; Received in revised form 14 March 2026; Accepted 15 March 2026

and logistic resources, increasing the demand for cost-effective and scalable approaches (Caputo and Manica, 2020).

To address these challenges, statistical modelling has emerged in the past two decades as an effective tool for predicting the geographic distribution and phenology of the species (Lippi et al., 2023). Spatio-temporal analysis, in particular, plays an important role in vector-borne disease surveillance by enabling decision-makers to allocate resources effectively and respond to outbreaks (Desjardins et al., 2018). Among the various statistical approaches, ecologists often employ correlative models to infer species phenology and spatial–temporal variations. These models establish statistical relationships between a response variable (e.g., species abundance or presence-absence) and predominantly abiotic covariates (Guisan et al., 2017; Edwards and Crone, 2021; Torina et al., 2023).

Existing correlative models for estimating *Ae. albopictus* distribution vary in scope and complexity. Some models generate predictions without explicitly accounting for temporal and seasonal variability, not necessarily capturing population dynamics over time (Ding et al., 2018). Furthermore, many others focus on large-scale or global predictions (for example, see Kraemer et al. (2015) and Ding et al. (2018)), which, while valuable for broad epidemiological insights, may lack the spatial resolution necessary for practical, localised interventions. In this context, the work by Carrieri et al. (2023) represents a valuable contribution to the field, as it is one of the first attempts to apply a robust statistical framework to model *Ae. albopictus* egg abundance in the Emilia-Romagna region. Their study applied a Bayesian multimodel linear regression to estimate seasonal densities of *Ae. albopictus* eggs in the Emilia-Romagna region. While this approach relies on predefined equations and prior knowledge, requiring careful parameter estimation to ensure accuracy, it may be constrained by its underlying model structure.

Unlike parametric models that impose predefined relationships, machine learning (ML) identifies patterns directly from the data, which can be complex and non-linear, thus potentially reducing bias and improving predictive performance. Indeed, ML-based models have shown superior performance in predicting species distributions, identifying ecological niches, and modelling seasonal fluctuations (Chen et al., 2019; Bonannella et al., 2022; Ceia-Hasse et al., 2023; Oeser et al., 2024; Da Re et al., 2025). However, despite these advantages, ML models remain sensitive to the variability introduced by different algorithmic choices (Benkendorf and Hawkins, 2020; Bazzichetto et al., 2023; Da Re et al., 2024b), which may produce different results, therefore model selection plays a fundamental role in predictive accuracy (Araújo and New, 2007; Pearson et al., 2006; Marmion et al., 2009). To address these challenges, ensemble learning techniques have emerged as an effective strategy to enhance model robustness and accuracy. While traditional aggregation methods, such as simple and weighted averaging, have been widely used (Marmion et al., 2009; Hao et al., 2019), studies suggest that stacking, or stacked generalisation, offers superior performance (Araújo et al., 2005; Araújo and New, 2007). Here, stacking is adopted as a pragmatic design choice aimed at operational stability and predictive consistency, rather than algorithmic novelty.

This study aims to develop a stacked ML forecasting model that could directly support regional mosquito control efforts through the provision of predicted abundances for the upcoming active season. A fundamental practical challenge for any such system concerns the configuration of the training data: surveillance programmes differ substantially in how long they have been operating and how many monitoring stations they deploy. Local public health authorities seeking to implement comparable forecasting systems must therefore make pragmatic decisions about the temporal depth and spatial coverage of data that may be used to train a predictive model. To address this operational question, we draw on the georeferenced database of *Ae. albopictus* egg observations collected between 2010 and 2023 in Emilia-Romagna and evaluate model performance across a structured set of operational training-window scenarios that vary both the temporal depth and the spatial coverage of the input data.

More specifically, the configurations analysed here are designed to reflect realistic surveillance constraints, not to isolate the statistical effect of sample size per se. All training windows are temporally contiguous and immediately precede the evaluation period, a design chosen because operational forecasting systems typically rely on the most recent available data, and because newly established programmes are by definition constrained to whatever historical record they have accumulated at the time of deployment. Within this operational framing, the study pursues three objectives: (1) to characterise how model predictive performance varies across training-window scenarios that differ in temporal depth; (2) to characterise analogous variation across scenarios that differ in the fraction of sampling locations included; and (3) to generate short-term forecasts of mosquito egg distribution and abundance to support public health preparedness. Our results are especially informative for local public health authorities that are considering the launch of similar forecasting systems, as they provide concrete, operationally grounded guidance on the data configurations that can sustain reliable predictions.

2. Methodology

2.1. Ovitrap data

This study focuses on the Emilia-Romagna region in northern Italy, situated in the Po Valley (Fig. 1). Emilia-Romagna experiences a humid subtropical climate (Köppen Cfa) in the lowlands transitioning to temperate oceanic conditions (Cfb) at higher elevations (Nistor, 2016). Annual precipitation ranges from below 800 mm in the plains to 2000 mm in the Apennine foothills, with a bimodal distribution peaking in spring (April-May) and autumn (October-November). The region exhibits pronounced spatial climate variability driven by its geomorphology, which transitions from the Po River floodplain through intensively cultivated plains to the northern Apennine ridge, with strong altitudinal control on temperature and precipitation patterns (Nistor, 2016). This environmental heterogeneity, combined with dense urbanisation in lowland municipalities and extensive agricultural land use, creates diverse habitat availability for *Ae. albopictus* across the region.

Since 2010, regional authorities have monitored *Ae. albopictus* populations using ovitraps, which are dark water-filled containers equipped with a surface for mosquito egg deposition. These traps are used to obtain a proxy for mosquito egg-laying activity and are inspected biweekly following standardised local protocols. Egg counts provide a reliable measure of mosquito activity and serve as a key tool in the region's surveillance efforts.

Mosquito monitoring in Emilia-Romagna is coordinated by Local and Regional Public Health departments, with municipalities responsible for operational activities (Carrieri et al., 2011). The program involves ten municipalities deploying a total of 755 georeferenced ovitraps annually from late May (week 21) to early October (week 40). The locations of all the ovitraps are shown in Figure S1. During each survey, the status of each ovitrap is evaluated following the Regional Surveillance Operative protocol (Di Luca, 2022). If a trap is found dry or overturned, its deposition substrate (a masonite stick) is excluded, and the data point is recorded as missing (NA). The collected sticks are sent to the Regional Environmental Protection Agency laboratories, where mosquito eggs are identified and counted using a stereomicroscope. A quality control process is then applied to the egg count data (Carrieri et al., 2017). After passing the quality check, the data are published on the regional portal www.zanzaratigreonline.it.

For data integration into the machine learning model, the egg counts of *Ae. albopictus* collected through ovitraps were set as the target variable. Temporal resolution was standardised to a weekly period using the `spreader` function from the *dynamAedes* R package

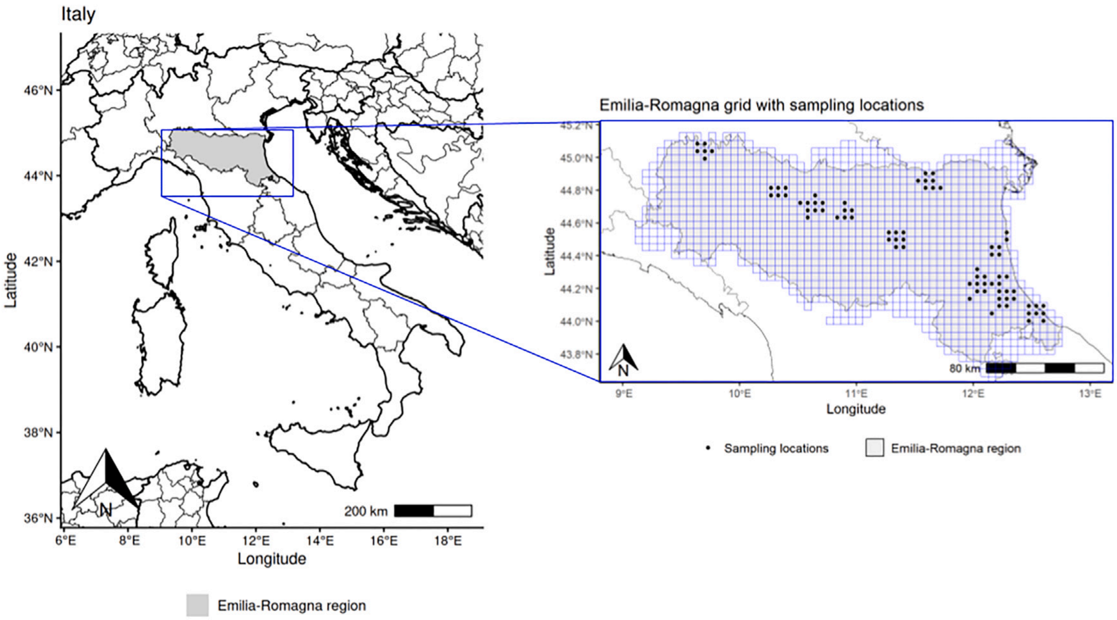

Fig. 1. Left: Location of Emilia-Romagna within Italy. Right: Grid used for aggregating ovitrap data, matching the resolution of the climatic datasets (approximately 5 × 5 km). Black dots indicate the sampling locations (SLs), representing the aggregated ovitrap data.

(Da Re et al., 2022). The spatial resolution (approximately 5 × 5 km) was set consistently with the meteorological dataset (Antolini et al., 2015). Ovitrap data were aggregated accordingly, with a similar pre-processing pipeline as the one described in Da Re et al. (2025), where the median egg count is calculated from the ovitraps available in each grid cell, referred to as a sampling location (SL) throughout this study. Each SL is identified by a unique numerical ID and represents the average egg observations within the grid cell. A total of 79 SLs are distributed across the study area.

2.2. Covariates

The study incorporates key environmental factors known to influence mosquito activity and development. Three primary covariates were included: air temperature, photoperiod (the number of daylight hours), and precipitation.

Air temperature is a dominant driver of mosquito physiology, influencing larval development rates, adult survival, and oviposition activity, and thus strongly constraining both the timing and magnitude of seasonal abundance (Toma et al., 2003; Roiz et al., 2010; Becker et al., 2020). Photoperiod provides a stable seasonal cue that regulates diapause induction and termination in *Ae. albopictus*, thereby shaping the onset and cessation of oviposition independently of short-term climatic variability (Roiz et al., 2011; Romiti et al., 2021; Carrieri et al., 2023). Precipitation influences the availability and persistence of breeding sites, particularly in urban environments where container habitats dominate, and modulates egg survival and larval success, albeit in a non-linear and context-dependent manner (Roiz et al., 2010; da Cruz Ferreira et al., 2017; Becker et al., 2020).

Daily air temperatures and precipitation data were extracted from ERG5, a meteorological dataset developed by the HydroMeteoClimate Service of Emilia-Romagna Regional Environmental Protection Agency (ARPAE). Currently, ERG5 covers the period from 2001 to the present and provides several spatially interpolated climate variables at a 5 × 5 km resolution based on data from ARPAE's meteorological network (Antolini et al., 2015), which is the standard adopted by the regional environmental authority for operational and environmental monitoring planning purposes.

To account for the delayed and cumulative effects of environmental conditions on mosquito populations, we derived rolling averages of each covariate, following the approach described in Da Re et al. (2025). Specifically, covariates were represented using rolling means to account for short-term temporal integration. Temperature and photoperiod variables were summarised as the median across the focal week (i) and the preceding one or two weeks (i–1, i–2), while precipitation variables were computed as the cumulative total over the same periods.

In addition to environmental variables, we incorporated seasonality and cyclic patterns via Fourier series using sine and cosine harmonics (Hyndman and Athanasopoulos, 2018). This approach outperforms dummy variables for high-frequency data, capturing annual trends with one harmonic pair and shorter-term seasonality with another. The four terms, added alongside other predictors, significantly improved the model's ability to capture cyclic fluctuations in median weekly egg counts.

To factor in the influence of urbanisation on mosquito distribution (Perrin et al., 2022) and to mitigate spatial sampling bias (Gutierrez-Velez and Wiese, 2020; Whitford et al., 2024), since monitoring sites are primarily located in major cities (Figure S1), we included a urbanisation index derived from the ESA CCI Land Cover database (www.esa-landcover-cci.org, Defourny et al. (2012)). This dataset provides annual gridded maps with 22 global land cover classes. Urban areas are coded as value 190, based on data from the Global Human Settlement Layer (Pesaresi et al., 2016) and the Global Urban Footprint (Esch et al., 2017). To construct the urbanisation index, we first extracted all pixels labelled as urban (value 190) to create a binary map (1 = urban, 0 = non-urban). We then rescaled this map from its original 1 km resolution to 5 km, calculating the proportion of urban cover within each grid cell using the `terra::zonal` function. The resulting index assigns each grid tile a value between 0 (completely non-urbanised) and 1 (fully urbanised), with annual updates reflecting changes over time.

Accounting for this urban zonation is particularly important given the well-established influence of urbanisation on *Ae. albopictus* distribution (Li et al., 2014; Manica et al., 2016; Westby et al., 2021; Torina et al., 2023), and the known risks that uncorrected spatial bias poses to model generalisability and inference (Reddy and Dávalos, 2003; Kadmon et al., 2004; Anderson and Gonzalez Jr., 2011; Kramer-Schadt et al., 2013; Yackulic et al., 2013).

2.3. Modelling framework

Stacking is an ensemble learning technique that combines predictions from multiple base models to mitigate overfitting and improve generalisability (Wolpert, 1992; Marmion et al., 2009). Unlike bagging or boosting, which focus on reducing variance or bias, stacking integrates diverse models, allowing a meta-learner to determine the optimal way to merge their outputs (Bonannella et al., 2022, 2023; Oeser et al., 2024). Building on the methodology described in Da Re et al. (2025), we implemented a stacked model using four machine learning algorithms as base learners: XGBoost (Chen and Guestrin, 2016), Random Forest (Breiman, 2001), Gradient Boosting Machine (Friedman, 2001), and Cubist (Kuhn et al., 2024). These models were then combined into a unified ensemble using a linear meta-learner, specifically a regularised linear regression model trained to optimally weight the base learners' predictions. This meta-model was implemented using the `mlr3` library (Bischl et al., 2016; Lang et al., 2019). The overall ensemble architecture is illustrated in Fig. 2(a).

To ensure consistent configuration and hence comparability across all base models, hyperparameters were optimised once using 10-fold cross-validation with 10 evaluations. However, we acknowledge the potential for overfitting by using this approach, particularly when training models on smaller datasets. These limitations are further explored in the "Discussion" section.

Once the ensemble was constructed and optimised via hyperparameter tuning, it underwent training, validation, and testing (Fig. 2(b)). Each base learner's predictions were assigned varying weights, reflecting their relative contributions to the final model output.

2.4. Operational training-window configurations

To assess how model performance varies with different configurations of training data, we applied a spatio-temporal subsampling strategy that is designed to mirror operational constraints. This involved iteratively selecting subsets of the dataset to create multiple training sets of varying sample sizes for each model, determined by the temporal depth of the available historical record and the fraction of sampling locations used. The training process covered four temporal windows, the longest spanning from 2011 to 2022, followed by progressively narrower timeframes (2015–2022, 2019–2022, and 2021–2022). For each period, five spatial fractions of the sampling locations (SLs), 0.10 (7 SLs), 0.25 (19 SLs), 0.50 (38 SLs), 0.75 (58 ± 1 SLs), and 0.90 (70 ± 1 SLs), were randomly sub-sampled from the full dataset. Each configuration was evaluated across five replications.

The choice to use contiguous, non-overlapping training windows that terminate immediately before the evaluation year was deliberate and grounded in operational surveillance practice. Operational forecasting systems for vector-borne disease surveillance are typically configured to use the most recently available data: predictions must be issued prospectively, meaning that only the historical record accumulated up to the forecast date can be used. In this context, non-contiguous or randomly sampled year combinations, while statistically valuable for assessing average model behaviour across diverse temporal conditions, do not reflect the data configurations that practitioners actually face when deploying or updating a surveillance model. Furthermore, the training windows were designed to represent a progression of operational scenarios corresponding to the natural maturation of a monitoring programme: a newly established system with two years of data (2021–2022), a system with moderate historical depth (four years: 2019–2022 and eight years: 2015–2022), and a temporally richer system with over a decade of data (twelve years: 2011–2022). This progression captures the operational question of our primary interest: how many years of monitoring data are needed before a regional forecasting system becomes reliably predictive? The accompanying spatial fractions similarly reflect scenarios ranging from a nascent, resource-limited network (10%, which in our case is 7 sampling locations) to a well-established programme with an extended spatial coverage (90%, 70 ± 1 sampling locations).

To validate the model, an internal validation was performed using 10-fold cross-validation within the training dataset; then, a spatial test was conducted on a separate dataset, using SLs that were excluded from training. For evaluating temporal transferability, model predictions were tested on all the available data from 2023, which was entirely withheld from the training of all 100 models.

2.5. Model performance evaluation

To quantify model performance, Root Mean Squared Error (RMSE) was computed for the internal, spatial, and temporal validations. RMSE quantifies prediction error in the original units of egg abundance (eggs per ovitrap-week), emphasising errors in high-abundance periods that are most relevant for vector control. Additionally, we computed relative RMSE (rRMSE), which is RMSE expressed as a percentage of the observed value range, which allows for easier interpretation across varying scales of mosquito abundance. Computations of both RMSE and rRMSE were restricted to monitoring weeks 20–45 (late May to early October), as these represent the active egg-laying season for *Ae. albopictus* in Emilia-Romagna and align with the available observations, ensuring an assessment that avoids extrapolation to unmonitored periods. The model with the lowest RMSE was selected to generate prediction maps for *Ae. albopictus* abundance and distribution in 2023.

To further analyse RMSE variations, we assessed main effects and interaction effects using a model in which RMSE was set as the response variable, with the explanatory variables training years, the fraction of sampling locations, and their interaction. An Analysis of Variance (ANOVA) was then conducted using a two-way model to evaluate statistical significance. Model comparisons were based on the Akaike Information Criterion (AIC) (Table S1), and descriptive statistics were calculated for RMSE across temporal windows and spatial fractions. Finally, Tukey's Honestly Significant Difference (HSD) test was performed for post-hoc comparisons.

3. Results

Among the base learners, the predictions from the Random Forest model had the largest positive influence on average, followed by GBM, XGBoost and Cubist (Figures S2 and S3). Temperature-related variables consistently emerged as the most influential factors across the models (Figure S4). These were followed by photoperiod variables, a sine Fourier harmonic, urbanisation, and precipitation with a 3-week lag. Ranked lower in importance were, in order, another sine Fourier harmonic, precipitation, and the cosine Fourier harmonics.

3.1. Internal cross-validation

For the internal 10-fold cross-validation set, which was used for hyperparameter tuning of the base models, RMSE values generally decreased as both the fraction of sampling locations and the temporal depth of the training window increased, though this trend was not entirely consistent (Table 1).

Cross-validation was not performed for the 0.10 sampling fraction (7 SLs) due to insufficient data. When executing the resampling procedure, an error was returned during model training and evaluation, which indicated that, for at least one fold, the resampling split produced an empty set. The issue arose because the resampling instance was instantiated on a task with too few rows to satisfy the requirements of the cross-validation strategy, leading to a failure in retrieving the necessary data from the backend.

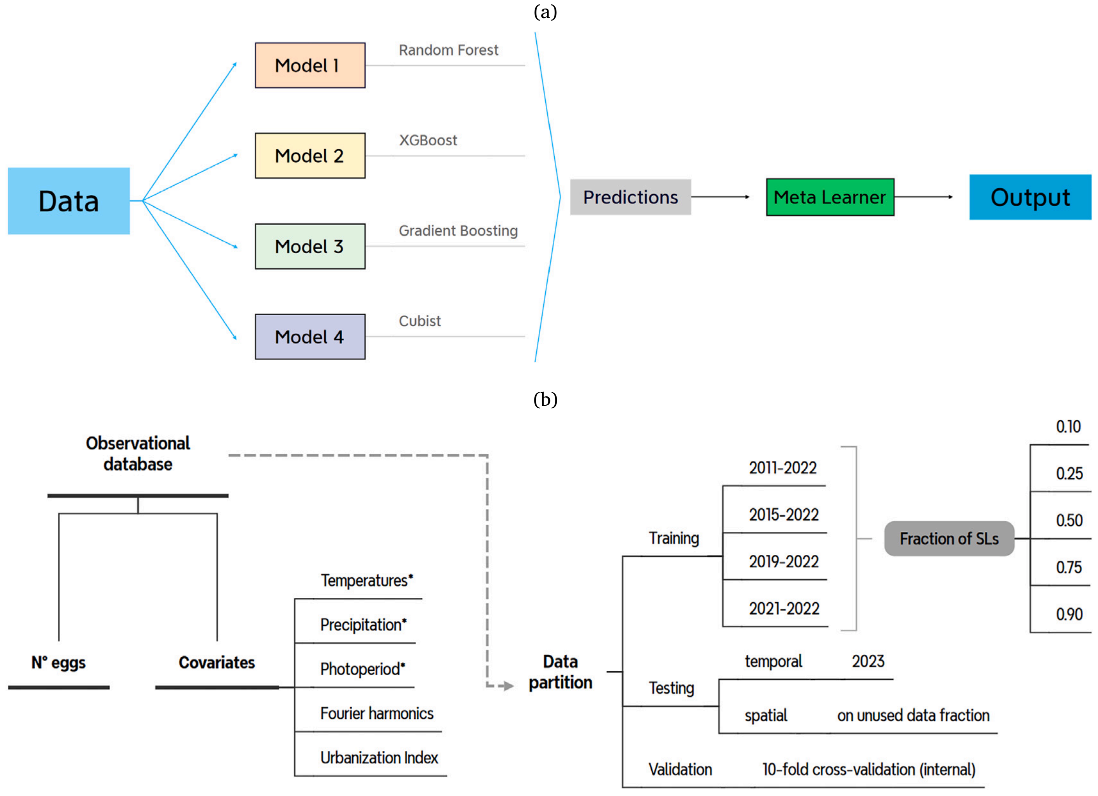

Fig. 2. (a) Stacked model architecture. (b) Map illustrating the components of the observational database and subsequent data splitting.

Table 1
Mean RMSE values with standard errors (±) for different training years and fractions of sampling locations for the internal cross-validation.

	2021–2022	2019–2022	2015–2022	2011–2022	Mean
0.25	90.48 ± 6.51	84.28 ± 1.29	81.70 ± 4.59	88.06 ± 3.72	86.13 ± 2.18
0.50	89.49 ± 3.38	85.58 ± 2.64	82.24 ± 1.00	79.41 ± 2.70	84.18 ± 1.47
0.75	88.24 ± 0.75	84.38 ± 1.91	88.63 ± 0.47	80.64 ± 1.66	85.47 ± 0.97
0.90	87.29 ± 0.91	85.06 ± 0.72	85.32 ± 0.94	79.41 ± 0.90	84.27 ± 0.78
Mean	88.87 ± 1.73	84.82 ± 0.83	84.47 ± 1.27	81.88 ± 1.41	

Table 2
Mean RMSE values with standard errors (±) for different training years and fractions of sampling locations for the spatial validation.

	2021–2022	2019–2022	2015–2022	2011–2022	Mean
0.10	101.49 ± 2.84	120.43 ± 2.88	106.71 ± 2.26	111.94 ± 2.39	110.15 ± 1.31
0.25	92.06 ± 2.68	97.91 ± 2.85	106.28 ± 2.91	100.92 ± 2.39	99.35 ± 1.36
0.50	89.02 ± 3.01	96.85 ± 3.58	99.23 ± 3.33	96.37 ± 3.32	95.41 ± 1.66
0.75	85.66 ± 5.15	97.69 ± 5.41	88.48 ± 3.76	89.95 ± 4.32	90.41 ± 2.35
0.90	90.30 ± 5.10	88.06 ± 8.08	93.79 ± 7.42	85.23 ± 4.94	89.35 ± 3.25
Mean	94.15 ± 1.54	105.40 ± 1.69	102.69 ± 1.46	102.25 ± 1.41	

3.2. Spatio-temporal validation

Across all temporal windows and fractions of SLs, the models demonstrated consistent performance on the spatial validation, with a comparable range and scale of the error (Table 2). When comparing model performance across specific training-window configurations, the two-year scenario (2021–2022) achieved the lowest mean RMSE overall (94.15), compared with the four-year (105.40), eight-year (102.69), and twelve-year (102.25) scenarios (Table 2). The lowest observed mean RMSE (85.23, Table 2) was produced by the twelve-year scenario at a 0.90 fraction, which has a very similar mean RMSE value to the two-year model at the 0.75 spatial fraction (85.66, Table 2). This model also achieved the lowest median RMSE (73.00, Table S3).

Relative RMSE (rRMSE), a scale-independent metric normalised to the observed data range, ranged from 16% to 24% across all configurations (Table S2), indicating good predictive performance relative to the empirical abundance variability (Li et al., 2013; Despotovic et al., 2016; McGough et al., 2017). rRMSE patterns mirror those already described for mean RMSE values, however we included it to facilitate the interpretation of the error values.

In Table 2 it is noticeable how there is a clear decreasing trend in RMSE as the fraction of data increases. In particular, the model trained with an SL of 0.90 had the lowest overall RMSE (89.35 ± 3.25). In Table S3, fractions of 0.10 and 0.25 generally show higher median RMSE values, with a wider spread (i.e., larger interquartile range and more outliers). This indicates more variability and less accuracy when fewer SLs are used for training. Fractions of 0.75 and 0.90 consistently produce lower RMSE values, with narrower boxplots (Figure S5) and fewer outliers, indicating better model performance and stability.

Two-way ANOVA (Table 3) confirmed that both temporal depth and spatial coverage had a highly significant effect on predictive accuracy ($p < 0.001$). With a Tukey HSD, we find out that the two-year configuration (2021–2022) differs significantly from all longer configurations, and no significant differences were detected among the 4-year, 8-year, and 12-year configurations (Table 4). Tukey HSD pairwise comparisons confirmed that all spatial fractions significantly outperformed the 0.10 fraction ($p < 0.05$), while differences among the 0.50, 0.75, and 0.90 fractions were not statistically significant (adjusted $p > 0.42$; Table 5). Therefore, configurations using 0.50–0.75 fractions (38–58 SLs) performed comparably. This plateau effect indicates that approximately half the available sampling locations are sufficient for near-optimal spatial validation performance under the evaluated conditions.

Table 3

Analysis of variance (two-way ANOVA) where the response variable is mean RMSE and the explanatory variables are the years of training and fraction of SLs.

	Degrees of freedom	Sum of squares	Mean square	F-value	p-value
Training years	3	67 581	22 527	10.23	<0.001
Fraction of SLs	4	210 176	52 544	23.986	<0.001
Residuals	3877	8 538 979	2 202		

Table 4

Tukey HSD test results for pairwise comparisons of the training years on mean RMSE, based on a two-way ANOVA model. The comparisons were conducted with a 95% confidence level. The lower and upper confidence intervals are reported in brackets (LCI, UCI).

Training years	Difference (LCI, UCI)	p-value
2015–2022–2011–2022	0.43 (−4.99, 5.86)	1.00
2019–2022–2011–2022	3.15 (−2.30, 8.60)	0.45
2021–2022–2011–2022	−8.10 (−13.55, −2.65)	<0.001
2019–2022–2015–2022	2.71 (−2.77, 8.20)	0.58
2021–2022–2015–2022	−8.54 (−14.02, −3.05)	<0.001
2021–2022–2019–2022	−11.25 (−16.76, −5.74)	<0.001

Table 5

Tukey HSD test results for pairwise comparisons of the fraction of SLs on mean RMSE, based on a two-way ANOVA model. The comparisons were conducted with a 95% confidence level. The lower and upper confidence intervals are reported in brackets (LCI, UCI).

Fraction of SLs	Difference (LCI, UCI)	p-value
0.25–0.10	−10.81 (−15.89, −5.73)	<0.001
0.50–0.10	−14.75 (−20.48, −9.02)	<0.001
0.75–0.10	−19.76 (−27.08, −12.43)	<0.001
0.90–0.10	−20.79 (−31.46, −10.11)	<0.001
0.50–0.25	−3.94 (−9.88, 1.99)	0.37
0.75–0.25	−8.95 (−16.43, −1.46)	<0.05
0.90–0.25	−9.98 (−20.76, 0.81)	0.085
0.75–0.50	−5.01 (−12.95, 2.93)	0.42
0.90–0.50	−6.04 (−17.14, 5.07)	0.57
0.90–0.75	−1.03 (−13.04, 10.98)	0.99

3.3. Predictions on the test set

The testing performed using the 2023 dataset showed similar error patterns across models trained with different periods and SL fractions (Figs. 3 and 4). Overall, the models tended to underestimate *Ae. albopictus* egg abundance in 2023, particularly during the peak summer months. This systematic underestimation was observed in both short-term (2021–2022) and longer-term models, though the timing of the seasonal peak was predicted accurately. Predictions for off-season months (e.g., late autumn) displayed relatively low variability for egg counts, expected to be 0, particularly for models trained on 12 years of data (Fig. 3). These longer-term models predicted fewer than 10 eggs per ovitrap in off-season months. The model trained on two years (2021–2022) demonstrated comparable performance to those trained on longer periods.

To test whether temporal proximity to the forecast year consistently improves performance, we conducted an auxiliary moving-window analysis in which eleven two-year windows spanning 2011–2022 were each trained on a fixed 75% spatial fraction, matching the lowest-RMSE spatial configuration (temporal window: 2021–2022; spatial fraction: 0.75) from our main analysis, and evaluated on the 2023 temporal test set. Each configuration was trained five times with independent random spatial subsets. The results confirmed a strong temporal gradient in predictive accuracy: the farthest windows performed substantially worse than more recent windows, with RMSE declining steeply towards the test year (Table S4 and Figure S7). The 2020–2021 window achieved the lowest median RMSE (69.9), followed closely by 2021–2022 (70.2).

3.4. Prediction maps

Spatial predictions for 2021 and 2022 were used to check if the predictions aligned with expected seasonal trends (Figure S6). However, it is important to note that these years overlap with the training years, meaning the model's predictions are based on data it was partially exposed to during training.

The prediction maps for 2023 were first generated using the best-performing model based on metrics of the spatial validation, which is composed by the unused SLs in training (Fig. 5(a)). The model successfully captured the trend of increasing egg abundance from spring to autumn, with predictions aligning with observed seasonal patterns in *Ae. albopictus* activity. Slight and spatially localised increases in abundance appear in urban centres in off-season months in the 12-year training configuration model. Moreover, using the model trained with the longest period and the largest fraction, a notable drop in egg abundance was predicted for mid-May 2023 (Fig. 5(b)), which coincides with the catastrophic flooding in the Romagna region during 15–17 May 2023 (Arrighi and Domeneghetti, 2023). Models trained on shorter temporal windows (2–4 years) or sparser spatial coverage (10%–50% of SLs) failed to reproduce this localised decline, instead predicting uninterrupted abundance increases across all municipalities (Fig. 5(a)).

4. Discussion

This study evaluated operational training configurations for a stacked machine-learning framework designed to forecast the weekly distribution and abundance of *Ae. albopictus* eggs in Emilia-Romagna. We assess which configurations can be effective to make reliable predictions under realistic surveillance constraints, and deployed the best-performing model in an operational public health platform. The results demonstrate that broad spatial coverage is a stronger driver of predictive accuracy than the temporal depth of the training window under the stable environmental and surveillance conditions of Emilia-Romagna (for comparative context of other *Ae. albopictus* surveillance programs, see Da Re et al., 2024a), and that models using only two temporally adjacent years of data can statistically match or exceed the performance of models trained on up to twelve years of historical records.

Operational contribution and comparison with existing approaches

Statistical models have been widely applied to estimate the distribution of *Ae. albopictus* (Lippi et al., 2023), but the majority of existing work focuses on habitat suitability on global or continental scales (Kraemer et al., 2015, 2019) and does not address the feasibility of producing operational near-real-time abundance forecasts within a regional surveillance context. Global and continental habitat suitability models are definitely valuable for assessing long-term invasion risk and guiding international responses and for predicting presence or absence. Regional studies such as Carrieri et al. (2023) have employed Bayesian frameworks to characterise weather-driven seasonal trends in egg density, providing important information on the influence of meteorological variables on *Ae. albopictus* population patterns; however, their outputs describe relative trends, beyond requiring parameterisation of species physiology. The present study advances this body of work by offering weekly abundance estimates expressed as median egg counts per ovitrap, directly actionable for scheduling anti-larval treatments and prioritising surveillance effort.

A concrete contribution of our model to the regional surveillance of the species is the integration of the model into a publicly accessible platform (www.zanzaratigreonline.it), developed in collaboration with the Emilia-Romagna Regional Health Authority. Further integration into a cyberinfrastructure could extend the platform to provide near-real-time forecasts with a two-week lead time, automated data

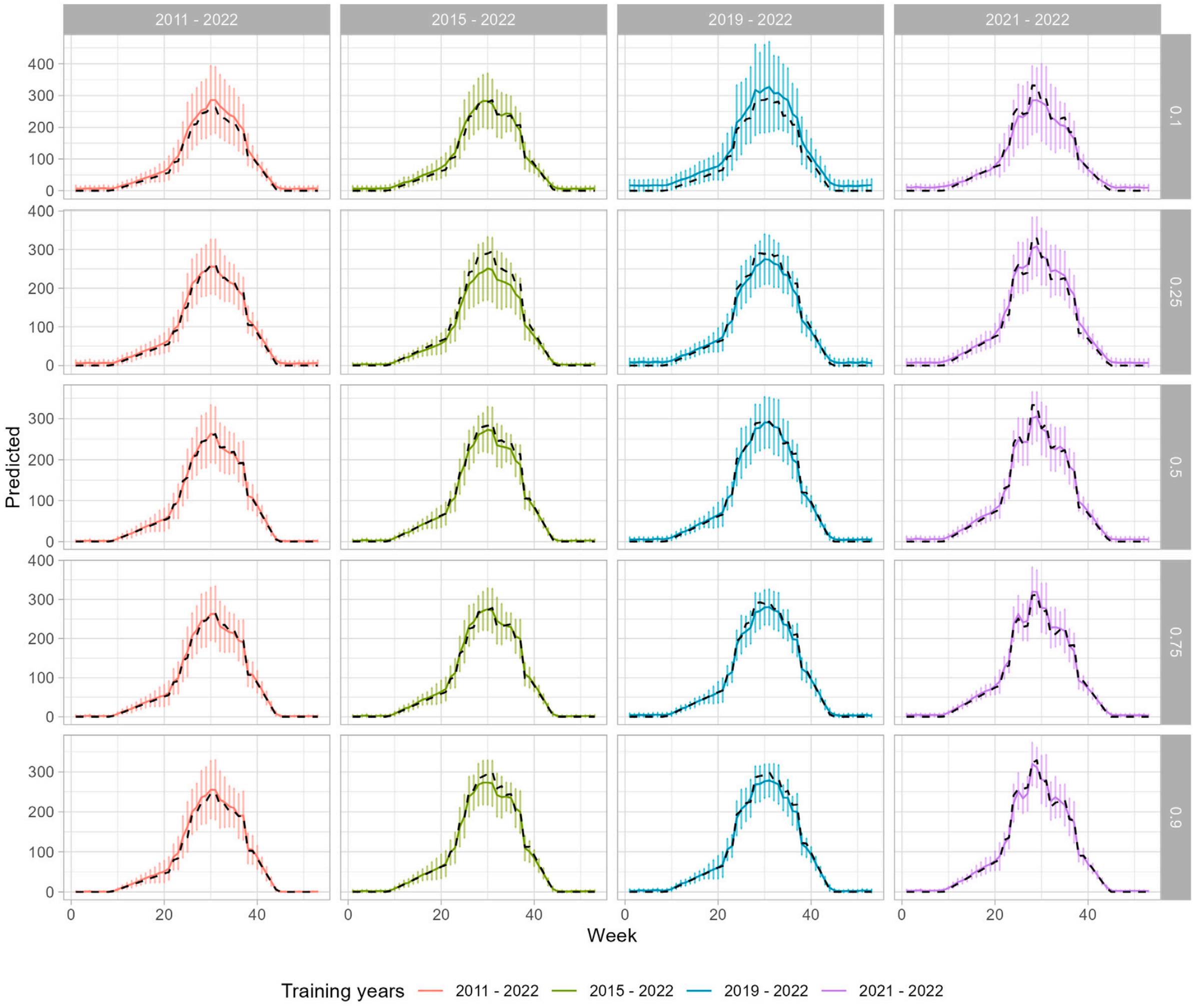

Fig. 3. Mean predicted (coloured lines) and mean observed (dashed lines) *Ae. albopictus* egg abundance for the spatial validation set across four temporal windows (2011–2022, 2015–2022, 2019–2022, and 2021–2022) and five data fractions (0.10, 0.25, 0.50, 0.75, and 0.90). Egg counts are aggregated at a weekly temporal resolution; curves are displayed as smoothed trends for visualisation purposes.

processing, and visualisation of historical trends and spatial distributions. Together, these developments position the framework as a scalable and transferable template for operational mosquito surveillance in other temperate European regions where *Ae. albopictus* is established or expanding (Benedict et al., 2007; Kraemer et al., 2019). These efforts set public health practice as a priority, which aligns with the United Nations Sustainable Development Goals 3 and 13, with a focus on ending vector-borne disease epidemics and enhancing early warning systems for global health risks (UN General Assembly, 2015). The stacked ensemble architecture, implemented here as a pragmatic strategy for stabilising predictions across heterogeneous environmental conditions, builds on established ensemble approaches in species distribution modelling (Araújo and New, 2007; Bonannella et al., 2022; Oeser et al., 2024) and extends them to a dynamic abundance-forecasting context.

Effect of spatial coverage on predictive accuracy

Model predictive accuracy improved consistently with the fraction of sampling locations included in training, with a statistically significant effect confirmed by two-way ANOVA ($p < 0.001$). Models trained on 90% of sampling locations (70 ± 1 SLs) achieved the lowest mean RMSE in the spatial validation, though configurations using 50%–75% of SLs (38–58 SLs) produced comparable results, suggesting a plateau in performance gains beyond approximately half of the available locations. Configurations using only 10% of SLs (7 SLs) showed statistically significant degradation relative to all others (Tukey HSD, $p < 0.05$), confirming that extreme spatial restriction compromises generalisation.

This pattern is consistent with the broader literature on spatial sampling sufficiency in ecological models. Recent work has explicitly attempted to define minimum sample size thresholds for reliable species distribution modelling. For example, Mitchel et al. (2025) used a simulated vector to quantify the optimal number of presence–absence records required for Random Forest models across European test sites, identifying thresholds of approximately 750–1000 observations for balanced datasets, with higher requirements for unbalanced samples. Their results emphasise that model reliability depends not only on algorithm choice but mostly on the sample size of the observations. In our study, the predictive performance plateaued when spatial coverage adequately represented the environmental gradient, suggesting that both sufficient sample size and sufficient spatial representativeness are necessary conditions for robust vector modelling, but that gains from increasing sampling effort may diminish once environmental heterogeneity is adequately captured.

When the spatial coverage is constrained, the model is exposed to a narrower range of environmental conditions and may fail to capture the full spectrum of spatial heterogeneity relevant for prediction (Randin et al., 2006; Ramampiandra et al., 2023). In the Emilia-Romagna

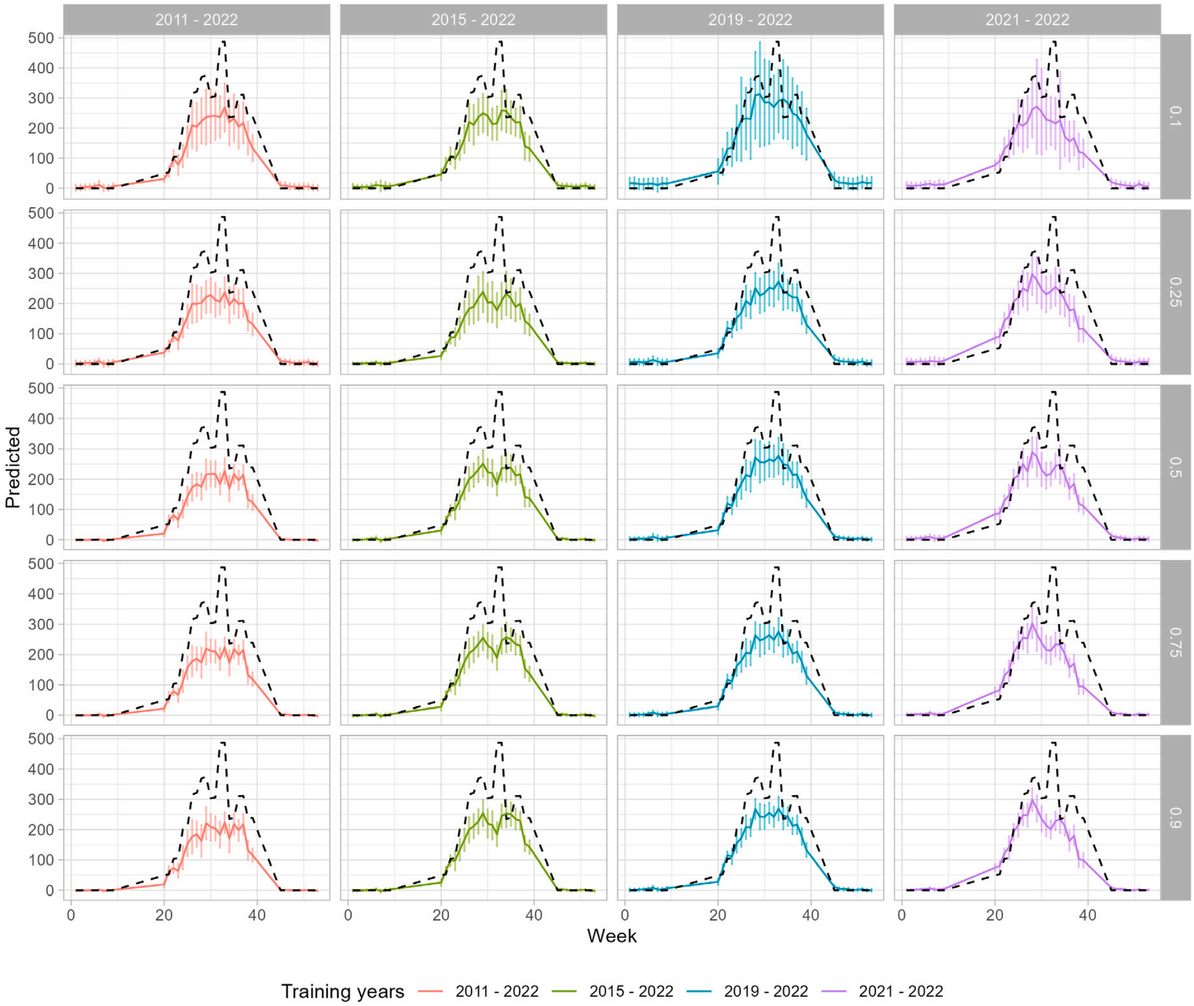

Fig. 4. Mean predicted (coloured lines) and mean observed (dashed lines) *Ae. albopictus* egg abundance for the temporal validation (year 2023) across four temporal windows (2011–2022, 2015–2022, 2019–2022, and 2021–2022) and five data fractions (0.10, 0.25, 0.50, 0.75, and 0.90). Egg counts are aggregated at a weekly temporal resolution; curves are displayed as smoothed trends for visualisation purposes.

network, where monitoring sites are concentrated in urbanised municipalities, sparse spatial sub-samples risk over-representing a narrow segment of the landscape gradient, amplifying the sampling bias that the urbanisation index was included to partially address (Gutierrez-Velez and Wiese, 2020; Whitford et al., 2024). The observation that intermediate spatial coverage (50%–75%) performs nearly as well as near-complete coverage suggests that local public health authorities establishing new surveillance programmes can achieve operationally adequate predictions with roughly half the spatial infrastructure of Emilia-Romagna, provided that the selected locations span the relevant environmental gradient.

Model performance across temporal training configurations

In our results, the two-year training configuration (2021–2022) achieved the lowest mean RMSE, performing statistically better than configurations with longer temporal windows. Conventional machine-learning knowledge anticipates improved performance with larger training samples (Goodfellow, 2016), however it is important to interpret this result within the specific design of the temporal subsampling and its inherent constraints. Indeed, the temporal configurations evaluated here were designed as a structured set of operationally motivated configurations in which all training windows are temporally contiguous and terminate immediately before the evaluation year. This design was chosen to reflect the conditions faced by a local public health authority deploying a forecasting system, where the most recently accumulated historical record is available. As a consequence of this design, the temporal configurations differ simultaneously in total data volume, historical depth, and inter-annual climatic diversity. Observed differences in predictive performance therefore cannot be attributed exclusively to the amount of data used for training and should not be interpreted as evidence that fewer years of data are intrinsically advantageous.

Several factors specific to these configurations may explain why the two-year scenario performed well under the conditions evaluated here. First, because the 2021–2022 window immediately precedes the evaluation year, it reflects recent environmental baselines and population dynamics with minimal distributional shift. This is a form of “operational recency” that benefits near-term forecasting. Second, longer training windows encompass a wider range of inter-annual climatic variability, which can be beneficial for robustness in dynamic systems but may introduce noise relative to conditions in the forecast year. This result is consistent with the variance–bias trade-off (Bishop and Nasrabadi, 2006; Hastie, 2009; Boehmke and Greenwell, 2019), where models trained on more variable datasets may exhibit higher variance in predictions, increasing RMSE on a temporally adjacent evaluation set even if their long-run generalisation is superior.

The pattern of our auxiliary analysis on the proximity of the temporal window to the test year, where error declined with training years closer to the test year (Table S4 and Figure S7), validates our

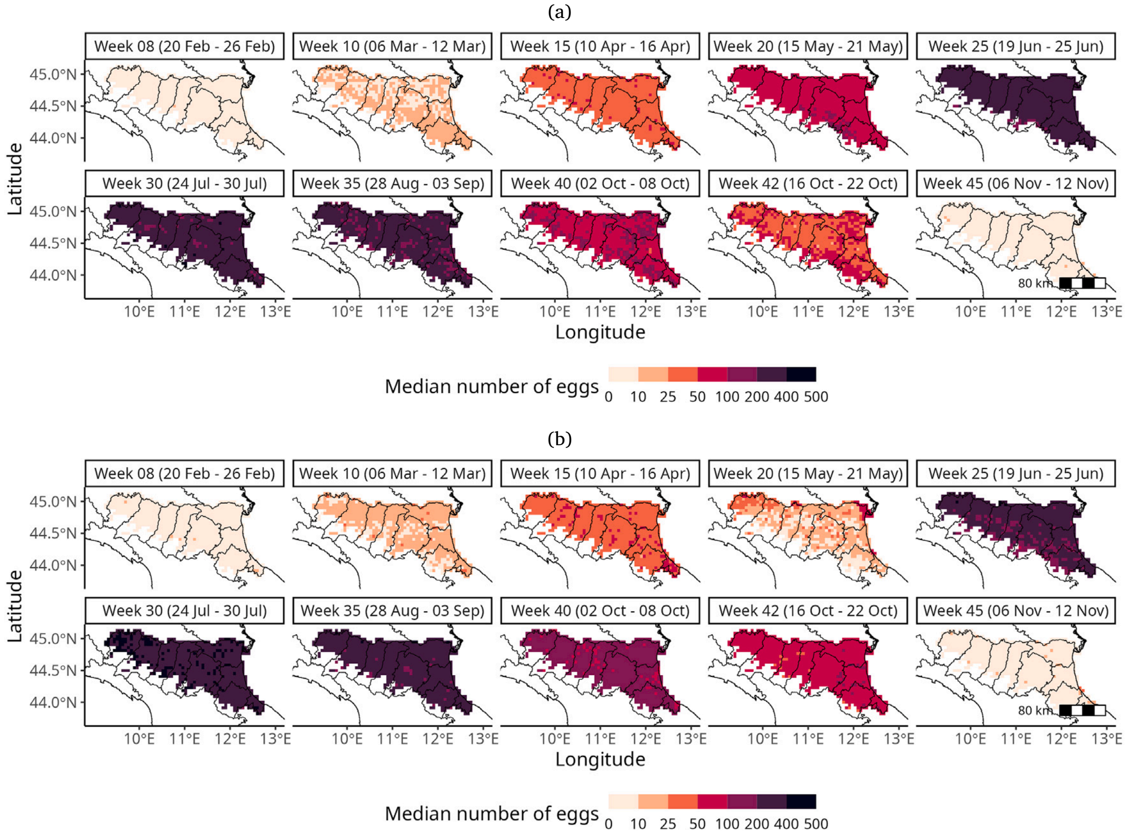

Fig. 5. Prediction map showing the distribution and abundance of *Ae. albopictus* eggs over 10 weeks in 2023. The model used to develop image (a) was trained using data from 2021–2022 and 0.75 of the SLs, while for (b) training was done on years 2011–2022 and 0.90 of the SLs.

operational strategy of using the most recently available training data while demonstrating that recency effects exhibit diminishing returns beyond approximately 3–4 years of temporal proximity. The strong performance of the 2014–2015 window, despite being 8–9 years removed from the forecast year, indicates that period-specific characteristics can also contribute to predictive accuracy, consistent with the variance–bias considerations discussed above.

Seasonal dynamics, abundance predictions, and phenological inference

The models correctly reproduced the seasonal pattern of *Ae. albopictus* egg abundance across all training configurations, with near-zero predictions during the off-season (late autumn and winter) and a broad abundance peak centred on mid-summer. The leading role of temperature-related covariates and photoperiod variables in model feature importance (Figure S4) is ecologically coherent and consistent with established findings on the thermal and photoperiodic control of *Ae. albopictus* population dynamics (Becker et al., 2020).

Overall, our model successfully predicted the seasonal timing of mosquito egg abundance, even though they underestimated the peak magnitudes during the summer months for 2023 (Fig. 4). Accurate prediction of seasonal timing is important for anticipating vector activity and guiding public health interventions. Nevertheless, the underestimation of peak abundance may reflect limitations in the model's ability to fully capture population dynamics during periods of high mosquito activity. We examined the distribution of egg counts used for model training (Figure S8), and obtained a strongly right-skewed distribution, with a large proportion of observations concentrated at low values (including a substantial fraction of zero counts) and only a small fraction of observations corresponding to high-abundance conditions. Because the model is trained by minimising a global loss function, predictive performance is dominated by the most frequently observed conditions. Additionally, 2023 has a longer upper tail of egg abundance distribution (Figure S9), so upper-tail events remain comparatively underrepresented in the training data. Therefore, a factor contributing to this behaviour of the model could be a bias towards the observed mean of the training dataset, which could have lead to the smoothing of extreme values, which is a well-documented tendency in machine learning literature (Zhang and Lu, 2012; Nguyen et al., 2015; Song, 2015; Hooker and Mentch, 2018; Ghosal and Hooker, 2020). This bias can be evident in ensemble methods, particularly those that rely on averaging across multiple models, such as bagging approaches (e.g. Random Forests). This averaging effect tends to shrink the prediction range, resulting in a narrower spread of values compared to the actual variability in the response variable (Meinshausen and Ridgeway, 2006; Zhang and Lu, 2012; Frame et al., 2022). Consequently, lower values are often overestimated, whereas higher values, such as peaks in abundance, are underestimated. In the case of stacking, this effect can be primarily observed if the meta-learner assigns a dominant weight to models prone to smoothing extreme values, such as tree-based ensembles like Random Forests — exactly what happened in this study. However, if the highest-weighted model within the ensemble is one that better captures extreme values, such as quantile regression models (Meinshausen and Ridgeway, 2006), simple neural networks or deep learning-based models — this effect may be less pronounced or absent. While such alternative base models might potentially mitigate this bias by better capturing extreme values, their influence in this specific context remains unexplored due to computational constraints. Future research could systematically evaluate the role of different base learners in stacking, testing whether models optimised for capturing extreme values improve predictions of peak abundance. Additionally, hybrid modelling approaches that integrate process-based models with machine learning could provide an alternative way to better represent population dynamics, particularly under conditions of high variability (Reichstein et al., 2019; Madzokere et al., 2020; Kraft et al., 2021; Steele et al., 2024; Acuña Espinoza et al., 2025).

Regarding the atypical abundance pattern observed in 2023, the twelve-year model with 90% spatial coverage successfully predicted the pronounced dip in egg abundance observed in the eastern municipalities in mid-May 2023 (Fig. 5(b)), which coincided with severe flooding in the eastern part of the region that could have affected reproductive and mortality rates (Harrington, 1995; Alto and Juliano, 2001; Medici et al., 2011; Dieng et al., 2012; Carrieri et al., 2023) of *Ae. albopictus*. This population reduction was observed exclusively in municipalities within the southeastern part of the region (Arrighi and Domeneghetti, 2023). Indeed, such flood events can disrupt *Ae. albopictus* larval development through multiple mechanisms: inundation flushes immature stages from container breeding sites, and subsequent mud accumulation can render manholes, drains, and other breeding habitats temporarily unsuitable (Arrighi and Domeneghetti, 2023; Koenraadt and Harrington, 2008; Roiz et al., 2015; Tran et al., 2013); additionally, larval mortality rates increase under high precipitation, while oviposition activity is suppressed during and immediately after flooding events (Harrington, 1995; Alto and Juliano, 2001; Dieng et al., 2012). The model trained on the adjacent two-years (2021–2022, Fig. 5(a)) possibly lacked exposure to comparable precipitation levels during training, and therefore was unable to reproduce this anomalous decline, making longer training windows more advantageous because they provide broader coverage of the environmental space, including infrequent conditions. It is important to note that while we used precipitation as a proxy for hydrological disturbance, we caution against over-interpreting the link of the predicted decline to the unusual precipitation.

Limitations and future directions

This study offers valuable insights into machine learning predictions of *Ae. albopictus* distribution and abundance in Emilia-Romagna, but there are limitations that indicate that further research could enhance the results. Model predictions generally matched observed seasonal egg abundance peaks in mid-summer, yet 2023 showed discrepancies, with observed egg counts fluctuating in ways not fully captured by predictions, which may be attributed to atypical environmental responses. Specifically, the observed mosquito egg abundance in 2023 seems less correlated with temperature and precipitation (Figure S10) compared to previous years (Figure S11), suggesting that possibly external factors beyond the selected covariates or unusual climatic events could have influenced mosquito dynamics.

Another possible source of variability is the impact of vector control measures. Pest control agencies are working to reduce the population of the species and minimise the nuisance caused by bites to the public (Ravasi et al., 2021). Detailed information about the timing and location of pest control treatments are unavailable, although regional authorities adhere to standard guidelines available in technical documents on www.zanzaratigreonline.it. However, the number of anti-larval treatment cycles varies across municipalities and the products used for vector control were changed in 2017 due to the emergence of resistance in *Culex pipiens* (Grigoraki et al., 2017), which may have influenced the effectiveness of the treatments and, consequently, the variability in observed egg abundance.

Hyperparameters for all 100 models were tuned once via 10-fold cross-validation to maintain uniformity in model configuration while maximising generalisation across different data subsets, but risked overfitting on small datasets, compounded by challenges in avoiding data leakage with spatiotemporal data (Roberts et al., 2017; Schratz et al., 2019; Kapoor and Narayanan, 2023). Partition-specific tuning could improve performance but it would also introduce a higher risk of overfitting due to reduced sample sizes in individual subsets.

Finally, occasionally models predicted high egg counts in unmonitored areas that are predominantly rural or mountaineous. Given that we cannot verify the accuracy of these predictions, as ovitraps are typically placed in urban areas at relatively low elevations, areas above 600 m were masked. Future enhancements could incorporate microclimate proxies like leaf area index (LAI) for shaded, humid conditions (Hardwick et al., 2015; De Frenne et al., 2019; Zellweger et al., 2019; Scheffers et al., 2014), alongside winter monitoring, since data collection occurs only between late May and early October, and integration of mechanistic models (for example, see Madzokere et al., 2020).

5. Conclusion

Extensive ovitrap data and associated environmental covariates have allowed the development of models capable of forecasting mosquito population dynamics with significant implications for public health management. Our findings indicate that models trained on extensive historical and spatial data captured broader environmental variability, which was particularly useful under unusual conditions. Moreover, it is clear that models that were trained on a higher fraction of sampling locations consistently produced more accurate predictions, emphasising the value of comprehensive spatial coverage of the monitoring. Interestingly, even short recent training windows produce reliable abundance predictions under similar climatic conditions, proving that decades of data are not essential for operational implementation.

The results help enhance mosquito surveillance and control strategies through the operational application of the developed predictive models in initiatives intending to reduce the risk of mosquito-borne diseases in both Emilia-Romagna and other regions facing similar challenges. Indeed, accurate, short-term forecasts of *Ae. albopictus* populations can guide targeted interventions, helping public health authorities allocate resources more efficiently, particularly in high-risk urban areas. A passive surveillance system is currently being developed to integrate ovitrap data with environmental factors, providing near real-time tracking and short-term forecasts of *Ae. albopictus* populations, aiming to enhance vector monitoring and support evidence-based mosquito control in Emilia-Romagna and potentially beyond.

CRediT authorship contribution statement

Margo Blaha: Writing – review & editing, Writing – original draft, Visualization, Validation, Software, Methodology, Formal analysis, Data curation, Conceptualization. **Alessandro Albieri:** Writing – review & editing, Validation, Resources, Funding acquisition, Data curation. **Paola Angelini:** Resources, Funding acquisition. **Gabriele Antolini:** Writing – review & editing. **Carmelo Bonannella:** Writing – review & editing, Methodology, Formal analysis. **Fabrizio Laurini:** Writing – review & editing, Methodology. **Roberto Rosà:** Writing – review & editing, Supervision, Resources, Project administration, Methodology, Funding acquisition, Formal analysis, Conceptualization. **Daniele Da Re:** Writing – review & editing, Validation, Supervision, Project administration, Methodology, Formal analysis, Conceptualization.

Declaration of competing interest

The authors declare that they have no known competing financial interests or personal relationships that could have appeared to influence the work reported in this paper.

Acknowledgements

This research was supported by PRIN "MosqIT" funding. We thank the local and regional public health authorities in Emilia-Romagna for their assistance in coordinating the mosquito monitoring program and providing access to ovitrap data. This work has also been developed in collaboration with the Open-Earth-Monitor Cyberinfrastructure project. The Open-Earth-Monitor Cyberinfrastructure project has received funding from the European Union's Horizon Europe research and innovation program under grant agreement No. 101059548. We also thank Dr. Emily Louise Pascoe for her careful revision and helpful suggestions to improve the fluency of the manuscript.

Appendix A. Supplementary data

Supplementary material related to this article can be found online at https://doi.org/10.1016/j.ecoinf.2026.103718.

Data availability

The code and data used throughout the study are available in a GitHub repository at www.github.com/margoblaha/StackedER.

References

Acuña Espinoza, Eduardo, Loritz, Ralf, Kratzert, Frederik, Klotz, Daniel, Gauch, Martin, Álvarez Chaves, Manuel, Ehret, Uwe, 2025. Analyzing the generalization capabilities of a hybrid hydrological model for extrapolation to extreme events. Hydrol. Earth Syst. Sci. 29 (5), 1277–1294.

Alto, Barry W., Juliano, Steven A., 2001. Precipitation and temperature effects on populations of Aedes albopictus (Diptera: Culicidae): implications for range expansion. J. Med. Entomol. 38 (5), 646–656.

Anderson, Robert P., Gonzalez Jr., Israel, 2011. Species-specific tuning increases robustness to sampling bias in models of species distributions: an implementation with Maxent. Ecol. Model. 222 (15), 2796–2811.

Angelini, P., Macini, P., Finarelli, A.C., Po, C., Venturelli, C., Bellini, R., Dottori, M., 2008. Chikungunya epidemic outbreak in Emilia-Romagna (Italy) during summer 2007. Parassitologia 50 (1/2), 97.

Antolini, G., Pavan, V., Tomozeiu, R., Tomei, F., Auteri, L., Marletto, V., Servizio-Idro-Meteo-Clima, ARPA-ER, 2015. The daily gridded climatic data set.

Araújo, Miguel B., New, Mark, 2007. Ensemble forecasting of species distributions. Trends Ecol. Evolut. 22 (1), 42–47.

Araújo, Miguel B, Whittaker, Robert J, Ladle, Richard J, Erhard, Markus, 2005. Reducing uncertainty in projections of extinction risk from climate change. Glob. Ecol. Biogeogr. 14 (6), 529–538.

Arrighi, Chiara, Domeneghetti, Alessio, 2023. Brief communication: On the environmental impacts of 2023 flood in Emilia-Romagna (Italy). Nat. Hazards Earth Syst. Sci. Discuss. 2023, 1–10.

Barzon, Luisa, Gobbi, Federico, Capelli, Gioia, Montarsi, Fabrizio, Martini, Simone, Riccetti, Silvia, Sinigaglia, Alessandro, Pacenti, Monia, Pavan, Giacomina, Rassu, Mario, et al., 2021. Autochthonous dengue outbreak in Italy 2020: clinical, virological and entomological findings. J. Travel. Med. 28 (8), taab130.

Bazzichetto, Manuele, Lenoir, Jonathan, Da Re, Daniele, Tordoni, Enrico, Rocchini, Duccio, Malavasi, Marco, Barták, Vojtech, Sperandii, Marta Gaia, 2023. Sampling strategy matters to accurately estimate response curves' parameters in species distribution models. Glob. Ecol. Biogeogr. 32 (10), 1717–1729.

Becker, Norbert, Petrić, Dušan, Zgomba, Marija, Boase, Clive, Madon, Minoo B, Dahl, Christine, Kaiser, Achim, 2020. Mosquitoes: Identification, Ecology and Control. Springer Nature.

Benedict, Mark Q, Levine, Rebecca S, Hawley, William A, Lounibos, L Philip, 2007. Spread of the tiger: global risk of invasion by the mosquito Aedes albopictus. Vector-Borne Zoonotic Dis. 7 (1), 76–85.

Benkendorf, Donald J., Hawkins, Charles P., 2020. Effects of sample size and network depth on a deep learning approach to species distribution modeling. Ecol. Inform. 60, 101137.

Bischl, Bernd, Lang, Michel, Kotthoff, Lars, Schiffner, Julia, Richter, Jakob, Studerus, Erich, Casalicchio, Giuseppe, Jones, Zachary, 2016. Mlr: Machine learning in R. J. Mach. Learn. Res. 17 (170), 1–5.

Bishop, Christopher M., Nasrabadi, Nasser M., 2006. Pattern Recognition and Machine Learning, vol. 4. 4, Springer.

Boehmke, Brad, Greenwell, Brandon M., 2019. Hands-on Machine Learning with R. Chapman and Hall/CRC.

Boes, Kathryn E, Ribeiro, José MC, Wong, Alex, Harrington, Laura C, Wolfner, Mariana F, Sirot, Laura K, 2014. Identification and characterization of seminal fluid proteins in the Asian tiger mosquito, Aedes albopictus. PLoS Negl. Trop. Dis. 8 (6), e2946.

Bonannella, Carmelo, Hengl, Tomislav, Heisig, Johannes, Parente, Leandro, Wright, Marvin N, Herold, Martin, De Bruin, Sytze, 2022. Forest tree species distribution for europe 2000–2020: mapping potential and realized distributions using spatiotemporal machine learning. PeerJ 10, e13728.

Bonannella, Carmelo, Hengl, Tomislav, Parente, Leandro, de Bruin, Sytze, 2023. Biomes of the world under climate change scenarios: increasing aridity and higher temperatures lead to significant shifts in natural vegetation. PeerJ 11, e15593.

Brady, Oliver J., Hay, Simon I., 2019. The first local cases of Zika virus in Europe. Lancet 394 (10213), 1991–1992.

Branda, Francesco, Giovanetti, Marta, Ceccarelli, Giancarlo, Ciccozzi, Massimo, Scarpa, Fabio, 2024. ArboItaly: Leveraging open data for enhanced arbovirus surveillance in Italy. Front. Pharmacol. 15, 1459408.

Breiman, Leo, 2001. Random forests. Mach. Learn. 45, 5–32.

Canali, Massimo, Rivas-Morales, Stefano, Beutels, Philippe, Venturelli, Claudio, 2017. The cost of Arbovirus disease prevention in Europe: area-wide integrated control of tiger mosquito, Aedes albopictus, in Emilia-Romagna, Northern Italy. Int. J. Environ. Res. Public Health 14 (4), 444.

Caputo, Beniamino, Manica, Mattia, 2020. Mosquito surveillance and disease outbreak risk models to inform mosquito-control operations in Europe. Curr. Opin. Insect Sci. 39, 101–108.

Carrieri, Marco, Albieri, Alessandro, Angelini, Paola, Baldacchini, Flavia, Venturelli, Claudio, Zeo, Silvia Mascali, Bellini, Romeo, 2011. Surveillance of the chikungunya vector Aedes albopictus (Skuse) in Emilia-Romagna (northern Italy): Organizational and technical aspects of a large scale monitoring system. J. Vector Ecol. 36 (1), 108–116.

Carrieri, Marco, Albieri, Alessandro, Angelini, Paola, Soracase, Monica, Dottori, Michele, Antolini, Gabriele, Bellini, Romeo, 2023. Effects of the weather on the seasonal population trend of Aedes albopictus (Diptera: Culicidae) in Northern Italy. Insects 14 (11), 879.

Carrieri, Marco, Albieri, Alessandro, Urbanelli, Sandra, Angelini, Paola, Venturelli, Claudio, Matrangolo, Carmela, Bellini, Romeo, 2017. Quality control and data validation procedure in large-scale quantitative monitoring of mosquito density: the case of Aedes albopictus in Emilia-Romagna region, Italy. Pathog. Glob. Health 111 (2), 83–90.

Ceia-Hasse, Ana, Sousa, Carla A., Gouveia, Bruna R., Capinha, César, 2023. Forecasting the abundance of disease vectors with deep learning. Ecol. Inform. (ISSN: 1574-9541) 78, 102272. http://dx.doi.org/10.1016/j.ecoinf.2023.102272, URL: https://www.sciencedirect.com/science/article/pii/S1574954123003011.

Chen, Tianqi, Guestrin, Carlos, 2016. Xgboost: A scalable tree boosting system. In: Proceedings of the 22nd Acm Sigkdd International Conference on Knowledge Discovery and Data Mining. pp. 785–794.

Chen, Shi, Whiteman, Ari, Li, Ang, Rapp, Tyler, Delmelle, Eric, Chen, Gang, Brown, Cheryl L, Robinson, Patrick, Coffman, Maren J, Janies, Daniel, et al., 2019. An operational machine learning approach to predict mosquito abundance based on socioeconomic and landscape patterns. Landsc. Ecol. 34, 1295–1311.

da Cruz Ferreira, Danielle Andreza, Degener, Carolin Marlen, de Almeida Marques-Toledo, Cecilia, Bendati, Maria Mercedes, Fetzer, Liane Oliveira, Teixeira, Camila P, Eiras, Álvaro Eduardo, 2017. Meteorological variables and mosquito monitoring are good predictors for infestation trends of Aedes aegypti, the vector of dengue, chikungunya and Zika. Parasites Vectors 10, 1–11.

Da Re, Daniele, Marini, Giovanni, Bonannella, Carmelo, Laurini, Fabrizio, Manica, Mattia, Anicic, Nikoleta, Albieri, Alessandro, Angelini, Paola, Arnoldi, Daniele, Bertola, Federica, et al., 2025. Modelling the seasonal dynamics of aedes albopictus populations using a spatio-temporal stacked machine learning model. Sci. Rep. 15 (1), 3750.

Da Re, Daniele, Marini, Giovanni, Bonannella, Carmelo, Laurini, Fabrizio, Manica, Mattia, Anicic, Nikoleta, Albieri, Alessandro, Angelini, Paola, Arnoldi, Daniele, Blaha, Marharyta, et al., 2024a. VectAbundance: a spatio-temporal database of Aedes mosquitoes observations. Sci. Data 11 (1), 636.

Da Re, Daniele, Tordoni, Enrico, Lenoir, Jonathan, Rubin, Sergio, Vanwambeke, Sophie O, 2024b. Towards causal relationships for modelling species distribution. J. Biogeogr. 51 (5), 840–852.

Da Re, Daniele, Van Bortel, Wim, Reuss, Friederike, Müller, Ruth, Boyer, Sebastien, Montarsi, Fabrizio, Ciocchetta, Silvia, Arnoldi, Daniele, Marini, Giovanni, Rizzoli, Annapaola, et al., 2022. DynamAedes: a unified modelling framework for invasive Aedes mosquitoes. Parasites Vectors 15 (1), 414.

De Carli, Gabriella, Carletti, Fabrizio, Spaziante, Martina, Gruber, Cesare Ernesto Maria, Rueca, Martina, Spezia, Pietro Giorgio, Vantaggio, Valentina, Barca, Alessandra, De Liberato, Claudio, Romiti, Federico, et al., 2023. Outbreaks of autochthonous Dengue in Lazio region, Italy, August to September 2023: preliminary investigation. Eurosurveillance 28 (44), 2300552.

De Frenne, Pieter, Zellweger, Florian, Rodríguez-Sánchez, Francisco, Scheffers, Brett R, Hylander, Kristoffer, Luoto, Miska, Vellend, Mark, Verheyen, Kris, Lenoir, Jonathan, 2019. Global buffering of temperatures under forest canopies. Nat. Ecol. Evol. 3 (5), 744–749.

Defourny, Pierre, Kirches, G, Brockmann, C, Boettcher, M, Peters, M, Bontemps, S, Lamarche, C, Schlerf, M, Santoro, M, 2012. Land cover CCI. Prod. User Guid. 2 (325), 10–16.

Delatte, Hélène, Dehecq, JS, Thiria, J, Domerg, C, Paupy, Christophe, Fontenille, Didier, 2008. Geographic distribution and developmental sites of Aedes albopictus (Diptera: Culicidae) during a Chikungunya epidemic event. Vector-Borne Zoonotic Dis. 8 (1), 25–34.

Desjardins, M.R., Whiteman, A., Casas, I., Delmelle, E., 2018. Space-time clusters and co-occurrence of chikungunya and dengue fever in Colombia from 2015 to 2016. Acta Trop. 185, 77–85.

Despotovic, Milan, Nedic, Vladimir, Despotovic, Danijela, Cvetanovic, Slobodan, 2016. Evaluation of empirical models for predicting monthly mean horizontal diffuse solar radiation. Renew. Sustain. Energy Rev. 56, 246–260.

Di Luca, Marco, 2022. Surveillance of mosquitoes in Italy.

Dieng, Hamady, Rahman, GM Saifur, Abu Hassan, A, Che Salmah, MR, Satho, Tomomitsu, Miake, Fumio, Boots, Michael, Sazaly, AbuBakar, 2012. The effects of simulated rainfall on immature population dynamics of Aedes albopictus and female oviposition. Int. J. Biometeorol. 56, 113–120.

Ding, Fangyu, Fu, Jingying, Jiang, Dong, Hao, Mengmeng, Lin, Gang, 2018. Mapping the spatial distribution of Aedes aegypti and Aedes albopictus. Acta Trop. 178, 155–162.

Edwards, Collin B., Crone, Elizabeth E., 2021. Estimating abundance and phenology from transect count data with GLMs. Oikos 130 (8), 1335–1345.

Esch, Thomas, Heldens, Wieke, Hirner, Andreas, Keil, Manfred, Marconcini, Mattia, Roth, Achim, Zeidler, Julian, Dech, Stefan, Strano, Emanuele, 2017. Breaking new ground in mapping human settlements from space–The Global Urban Footprint. ISPRS J. Photogramm. Remote Sens. 134, 30–42.

Frame, Jonathan M, Kratzert, Frederik, Klotz, Daniel, Gauch, Martin, Shalev, Guy, Gilon, Oren, Qualls, Logan M, Gupta, Hoshin V, Nearing, Grey S, 2022. Deep learning rainfall-runoff predictions of extreme events. Hydrol. Earth Syst. Sci. 26 (13), 3377–3392.

Friedman, Jerome H., 2001. Greedy function approximation: a gradient boosting machine. Ann. Stat. 1189–1232.

Ghosal, Indrayudh, Hooker, Giles, 2020. Boosting random forests to reduce bias; one-step boosted forest and its variance estimate. J. Comput. Graph. Statist. 30 (2), 493–502.

Goodfellow, Ian, 2016. Deep Learning, vol. 196, MIT Press.

Grigoraki, Linda, Puggioli, Arianna, Mavridis, Konstantinos, Douris, Vassilis, Montanari, Mario, Bellini, Romeo, Vontas, John, 2017. Striking diflubenzuron resistance in Culex pipiens, the prime vector of West Nile Virus. Sci. Rep. 7 (1), 11699.

Guisan, Antoine, Thuiller, Wilfried, Zimmermann, Niklaus E., 2017. Habitat Suitability and Distribution Models: with Applications in R. Cambridge University Press.

Gutierrez-Velez, Victor Hugo, Wiese, Daniel, 2020. Sampling bias mitigation for species occurrence modeling using machine learning methods. Ecol. Inform. 58, 101091.

Hao, Tianxiao, Elith, Jane, Guillera-Arroita, Gurutzeta, Lahoz-Monfort, José J, 2019. A review of evidence about use and performance of species distribution modelling ensembles like BIOMOD. Diversity and Distributions 25 (5), 839–852.

Hardwick, Stephen R, Toumi, Ralf, Pfeifer, Marion, Turner, Edgar C, Nilus, Reuben, Ewers, Robert M, 2015. The relationship between leaf area index and microclimate in tropical forest and oil palm plantation: Forest disturbance drives changes in microclimate. Agricult. Forest. Meterol. 201, 187–195.

Harrington, Richard, 1995. Insects in a changing environment. Academic Press, London.

Hastie, Trevor, 2009. The elements of statistical learning: data mining, inference, and prediction.

Hooker, Giles, Mentch, Lucas, 2018. Bootstrap bias corrections for ensemble methods. Stat. Comput. 28, 77–86.

Hyndman, Rob J., Athanasopoulos, George, 2018. Forecasting: Principles and Practice. OTexts.

Kadmon, Ronen, Farber, Oren, Danin, Avinoam, 2004. Effect of roadside bias on the accuracy of predictive maps produced by bioclimatic models. Ecol. Appl. 14 (2), 401–413.

Kapoor, Sayash, Narayanan, Arvind, 2023. Leakage and the reproducibility crisis in machine-learning-based science. Patterns 4 (9).

Koenraadt, C.J.M., Harrington, L.C., 2008. Flushing effect of rain on container-inhabiting mosquitoes Aedes aegypti and Culex pipiens (Diptera: Culicidae). J. Med. Entomol. 45 (1), 28–35.

Kraemer, Moritz UG, Reiner Jr., Robert C, Brady, Oliver J, Messina, Jane P, Gilbert, Marius, Pigott, David M, Yi, Dingdong, Johnson, Kimberly, Earl, Lucas, Marczak, Laurie B, et al., 2019. Past and future spread of the arbovirus vectors Aedes aegypti and Aedes albopictus. Nat. Microbiol. 4 (5), 854–863.

Kraemer, Moritz UG, Sinka, Marianne E, Duda, Kirsten A, Mylne, Adrian QN, Shearer, Freya M, Barker, Christopher M, Moore, Chester G, Carvalho, Roberta G, Coelho, Giovanini E, Van Bortel, Wim, et al., 2015. The global distribution of the arbovirus vectors Aedes aegypti and Ae. albopictus. Elife 4, e08347.

Kraft, Basil, Jung, Martin, Körner, Marco, Koirala, Sujan, Reichstein, Markus, 2021. Towards hybrid modeling of the global hydrological cycle. Hydrol. Earth Syst. Sci. Discuss. 2021, 1–40.

Kramer-Schadt, Stephanie, Niedballa, Jürgen, Pilgrim, John D., Schröder, Boris, Lindenborn, Jana, Reinfelder, Vanessa, Stillfried, Milena, Heckmann, Ilja, Scharf, Anne K., Augeri, Dave M., Cheyne, Susan M., Hearn, Andrew J., Ross, Joanna, Macdonald, David W., Mathai, John, Eaton, James, Marshall, Andrew J., Semiadi, Gono, Rustam, Rustam, Bernard, Henry, Alfred, Raymond, Samejima, Hiromitsu, Duckworth, J.W., Breitenmoser-Wuersten, Christine, Belant, Jerrold L., Hofer, Heribert, Wilting, Andreas, 2013. The importance of correcting for sampling bias in MaxEnt species distribution models. Diversity and Distributions 19 (11), 1366–1379. http://dx.doi.org/10.1111/ddi.12096, eprint: https://onlinelibrary.wiley.com/doi/pdf/70310.1111/ddi.12096 URL: https://onlinelibrary.wiley.com/doi/abs/10.1111/ddi.12096.

Kuhn, Max, Weston, Steve, Keefer, Chris, 2024. Package 'Cubist'. Rule-and Instance-Based Regression Modeling. R Package Version 0.4 1.

Lang, Michel, Binder, Martin, Richter, Jakob, Schratz, Patrick, Pfisterer, Florian, Coors, Stefan, Au, Quay, Casalicchio, Giuseppe, Kotthoff, Lars, Bischl, Bernd, 2019. mlr3: A modern object-oriented machine learning framework in R. J. Open Source Softw. 4 (44), 1903.

Li, Yiji, Kamara, Fatmata, Zhou, Guofa, Puthiyakunnon, Santhosh, Li, Chunyuan, Liu, Yanxia, Zhou, Yanhe, Yao, Lijie, Yan, Guiyun, Chen, Xiao-Guang, 2014. Urbanization increases Aedes albopictus larval habitats and accelerates mosquito development and survivorship. PLoS Negl. Trop. Dis. 8 (11), e3301.

Li, Mao-Fen, Tang, Xiao-Ping, Wu, Wei, Liu, Hong-Bin, 2013. General models for estimating daily global solar radiation for different solar radiation zones in mainland China. Energy Convers. Manage. 70, 139–148.

Lippi, Catherine A, Mundis, Stephanie J, Sippy, Rachel, Flenniken, J Matthew, Chaudhary, Anusha, Hecht, Gavriella, Carlson, Colin J, Ryan, Sadie J, 2023. Trends in mosquito species distribution modeling: insights for vector surveillance and disease control. Parasites Vectors 16 (1), 302.

Madzokere, Eugene T, Hallgren, Willow, Sahin, Oz, Webster, Julie A, Webb, Cameron E, Mackey, Brendan, Herrero, Lara J, 2020. Integrating statistical and mechanistic approaches with biotic and environmental variables improves model predictions of the impact of climate and land-use changes on future mosquito-vector abundance, diversity and distributions in Australia. Parasites Vectors 13, 1–13.

Manica, Mattia, Filipponi, Federico, D'Alessandro, Antonello, Screti, Alessia, Neteler, Markus, Rosa, Roberto, Solimini, Angelo, Della Torre, Alessandra, Caputo, Beniamino, 2016. Spatial and temporal hot spots of Aedes albopictus abundance inside and outside a south European metropolitan area. PLoS Negl. Trop. Dis. 10 (6), e0004758.

Marmion, Mathieu, Parviainen, Miia, Luoto, Miska, Heikkinen, Risto K, Thuiller, Wilfried, 2009. Evaluation of consensus methods in predictive species distribution modelling. Diversity and Distributions 15 (1), 59–69.

McGough, Sarah F., Brownstein, John S., Hawkins, Jared B., Santillana, Mauricio, 2017. Forecasting Zika incidence in the 2016 Latin America outbreak combining traditional disease surveillance with search, social media, and news report data. PLoS Negl. Trop. Dis. 11 (1), e0005295.

Medici, Anna, Carrieri, Marco, Scholte, Ernst-Jan, Maccagnani, Bettina, Luisa Dindo, Maria, Bellini, Romeo, 2011. Studies on Aedes albopictus larval mass-rearing optimization. J. Econ. Entomol. 104 (1), 266–273.

Meinshausen, Nicolai, Ridgeway, Greg, 2006. Quantile regression forests. J. Mach. Learn. Res. 7 (6).

Mitchel, Lianne, Hendrickx, Guy, MacLeod, Ewan T, Marsboom, Cedric, 2025. Predicting vector distribution in Europe: at what sample size are species distribution models reliable? Front. Vet. Sci. 12, 1584864.

Nguyen, Thanh-Tung, Huang, Joshua Z., Nguyen, Thuy Thi, 2015. Two-level quantile regression forests for bias correction in range prediction. Mach. Learn. 101, 325–343.

Nistor, Mărgărit M., 2016. Spatial distribution of climate indices in the Emilia-Romagna region. Meteorol. Appl. 23 (2), 304–313.

Oeser, Julian, Zurell, Damaris, Mayer, Frieder, Çoraman, Emrah, Toshkova, Nia, Deleva, Stanimira, Natradze, Ioseb, Benda, Petr, Ghazaryan, Astghik, Irmak, Sercan, et al., 2024. The best of two worlds: Using stacked generalisation for integrating expert range maps in species distribution models. Glob. Ecol. Biogeogr. e13911.

Pearson, Richard G, Thuiller, Wilfried, Araújo, Miguel B, Martinez-Meyer, Enrique, Brotons, Lluís, McClean, Colin, Miles, Lera, Segurado, Pedro, Dawson, Terence P, Lees, David C, 2006. Model-based uncertainty in species range prediction. J. Biogeogr. 33 (10), 1704–1711.

Perrin, Antoine, Glaizot, Olivier, Christe, Philippe, 2022. Worldwide impacts of landscape anthropization on mosquito abundance and diversity: A meta-analysis. Global Change Biol. 28 (23), 6857–6871.

Pesaresi, Martino, Ehrlich, Daniele, Ferri, Stefano, Florczyk, Aneta J, Freire, Sergio, Halkia, Matina, Julea, Andreea, Kemper, Thomas, Soille, Pierre, Syrris, Vasileios, et al., 2016. Operating Procedure for the Production of the Global Human Settlement Layer from Landsat Data of the Epochs 1975, 1990, 2000, and 2014. Publications Office of the European Union Luxembourg.

Ramampiandra, Emma Chollet, Scheidegger, Andreas, Wydler, Jonas, Schuwirth, Nele, 2023. A comparison of machine learning and statistical species distribution models: Quantifying overfitting supports model interpretation. Ecol. Model. (ISSN: 0304-3800) 481, 110353. http://dx.doi.org/10.1016/j.ecolmodel.2023.110353, URL: https://www.sciencedirect.com/science/article/pii/S0304380023000819.

Randin, Christophe F, Dirnböck, Thomas, Dullinger, Stefan, Zimmermann, Niklaus E, Zappa, Massimiliano, Guisan, Antoine, 2006. Are niche-based species distribution models transferable in space? J. Biogeogr. 33 (10), 1689–1703.

Ravasi, Damiana, Parrondo Monton, Diego, Tanadini, Matteo, Flacio, Eleonora, 2021. Effectiveness of integrated Aedes albopictus management in southern Switzerland. Parasites Vectors 14, 1–15.

Reddy, Sushma, Dávalos, Liliana M., 2003. Geographical sampling bias and its implications for conservation priorities in Africa. J. Biogeogr. 30 (11), 1719–1727.

Reichstein, Markus, Camps-Valls, Gustau, Stevens, Bjorn, Jung, Martin, Denzler, Joachim, Carvalhais, Nuno, Prabhat, F, 2019. Deep learning and process understanding for data-driven Earth system science. Nature 566 (7743), 195–204.

Rezza, G., Nicoletti, L., Angelini, R., Romi, R., Finarelli, A.C., Panning, M., Cordioli, P., Fortuna, C., Boros, S., Magurano, F., et al., 2007. Infection with chikungunya virus in Italy: an outbreak in a temperate region. Lancet 370 (9602), 1840–1846.

Roberts, David R, Bahn, Volker, Ciuti, Simone, Boyce, Mark S, Elith, Jane, Guillera-Arroita, Gurutzeta, Hauenstein, Severin, Lahoz-Monfort, José J, Schröder, Boris, Thuiller, Wilfried, et al., 2017. Cross-validation strategies for data with temporal, spatial, hierarchical, or phylogenetic structure. Ecography 40 (8), 913–929.

Roiz, David, Boussès, Philippe, Simard, Frédéric, Paupy, Christophe, Fontenille, Didier, 2015. Autochthonous chikungunya transmission and extreme climate events in southern France. PLoS Negl. Trop. Dis. 9 (6), e0003854.

Roiz, David, Neteler, Markus, Castellani, Cristina, Arnoldi, Daniele, Rizzoli, Annapaola, 2011. Climatic factors driving invasion of the tiger mosquito (Aedes albopictus) into new areas of Trentino, northern Italy. PLoS One 6 (4), e14800.

Roiz, David, Rosà, Roberto, Arnoldi, Daniele, Rizzoli, Annapaola, 2010. Effects of temperature and rainfall on the activity and dynamics of host-seeking aedes albopictus females in northern Italy. Vector-Borne Zoonotic Dis. 10 (8), 811–816.

Romiti, Federico, Ermenegildi, Arianna, Magliano, Adele, Rombolà, Pasquale, Varrenti, Donatella, Giammattei, Roberto, Gasbarra, Silvia, Ursino, Simona, Casagni, Luca, Scriboni, Andrea, et al., 2021. Aedes albopictus (Diptera: Culicidae) monitoring in the Lazio region (central Italy). J. Med. Entomol. 58 (2), 847–856.

Sacco, Chiara, Liverani, Augusto, Venturi, Giulietta, Gavaudan, Stefano, Riccardo, Flavia, Salvoni, Giovanna, Fortuna, Claudia, Marinelli, Katia, Marsili, Giulia, Pesaresi, Alessia, et al., 2024. Autochthonous dengue outbreak in Marche Region, Central Italy, August to October 2024. Eurosurveillance 29 (47), 2400713.

Scheffers, Brett R, Edwards, David P, Diesmos, Arvin, Williams, Stephen E, Evans, Theodore A, 2014. Microhabitats reduce animals' exposure to climate extremes. Global Change Biol. 20 (2), 495–503.

Schratz, Patrick, Muenchow, Jannes, Iturritxa, Eugenia, Richter, Jakob, Brenning, Alexander, 2019. Hyperparameter tuning and performance assessment of statistical and machine-learning algorithms using spatial data. Ecol. Model. 406, 109–120.

Song, Jongwoo, 2015. Bias corrections for random forest in regression using residual rotation. J. Korean Statist. Soc. 44 (2), 321–326.

Steele, Hannah, Small, Eric E., Raleigh, Mark S., 2024. Demonstrating a hybrid machine learning approach for snow characteristic estimation throughout the western United States. Water Resour. Res. 60 (6).

Toma, Luciano, Severini, Francesco, Di Luca, Marco, Bella, Antonino, Roberto, Romì, 2003. Seasonal patterns of oviposition and egg hatching rate of Aedes albopictus in Rome. J. Am. Mosq. Control Assoc. 19 (1), 100.

Torina, Alessandra, La Russa, Francesco, Blanda, Valeria, Peralbo-Moreno, Alfonso, Casades-Martí, Laia, Di Pasquale, Liliana, Bongiorno, Carmelo, Badaco, Valeria Vitale, Toma, Luciano, Ruiz-Fons, Francisco, 2023. Modelling time-series Aedes albopictus abundance as a forecasting tool in urban environments. Ecol. Indic. 150, 110232.

Tran, Annelise, L'ambert, Grégory, Lacour, Guillaume, Benoît, Romain, Demarchi, Marie, Cros, Myriam, Cailly, Priscilla, Aubry-Kientz, Mélaine, Balenghien, Thomas, Ezanno, Pauline, 2013. A rainfall-and temperature-driven abundance model for Aedes albopictus populations. Int. J. Environ. Res. Public Health 10 (5), 1698–1719.

UN General Assembly, 2015. Transforming our World: The 2030 Agenda for Sustainable Development, 21 October 2015. Tech. rep. A/RES/70/1.

Venturi, Giulietta, Di Luca, Marco, Fortuna, Claudia, Remoli, Maria Elena, Riccardo, Flavia, Severini, Francesco, Toma, Luciano, Del Manso, Martina, Benedetti, Eleonora, Caporali, Maria Grazia, et al., 2017. Detection of a chikungunya outbreak in Central Italy, August to September 2017. Eurosurveillance 22 (39), 17–00646.

Westby, Katie M, Adalsteinsson, Solny A, Biro, Elizabeth G, Beckermann, Alexis J, Medley, Kim A, 2021. Aedes albopictus populations and larval habitat characteristics across the landscape: Significant differences exist between urban and rural land use types. Insects 12 (3), 196.

Whitford, Anna M., Shipley, Benjamin R., McGuire, Jenny L., 2024. The influence of the number and distribution of background points in presence-background species distribution models. Ecol. Model. 488, 110604.

Wolpert, David H., 1992. Stacked generalization. Neural Netw. 5 (2), 241–259.

Yackulic, Charles B, Chandler, Richard, Zipkin, Elise F, Royle, J Andrew, Nichols, James D, Campbell Grant, Evan H, Veran, Sophie, 2013. Presence-only modelling using MAXENT: when can we trust the inferences? Methods Ecol. Evol. 4 (3), 236–243.

Zellweger, Florian, De Frenne, Pieter, Lenoir, Jonathan, Rocchini, Duccio, Coomes, David, 2019. Advances in microclimate ecology arising from remote sensing. Trends Ecol. Evolut. 34 (4), 327–341.

Zhang, Guoyi, Lu, Yan, 2012. Bias-corrected random forests in regression. J. Appl. Stat. 39 (1), 151–160.